The Microsomal Enzyme 17β-Hydroxysteroid Dehydrogenase 3 Faces the Cytoplasm and Uses NADPH Generated by Glucose-6-Phosphate Dehydrogenase

Balázs Legeza, Zoltán Balázs, Lyubomir G. Nashev, and Alex Odermatt

Division of Molecular and Systems Toxicology, Department of Pharmaceutical Sciences, University of Basel, 4056 Basel, Switzerland

Recent studies proposed a functional coupling between 17β-hydroxysteroid dehydrogenase 3 (17β-HSD3)-dependent testosterone formation and 11β-hydroxysteroid dehydrogenase 1 (11β-HSD1)-mediated interconversion of glucocorticoids through competition for the luminal pyridine nucleotide pool. To test this hypothesis, we used human embryonic kidney-293 cells transfected with 17β-HSD3 and/or 11β-HSD1, in the absence or presence of hexose-6-phosphate dehydrogenase that generates reduced nicotinamide adenine dinucleotide phosphate (NADPH) in the endoplasmic reticulum and determined enzyme activities. As an endogenous cell model, mouse MA-10 Leydig cells were used. 17β-HSD3-dependent reduction of Δ4-androstene-3,17-dione was affected by neither coexpression with 11β-HSD1 nor overexpression or knockdown of hexose-6-phosphate dehydrogenase. In contrast, knockdown of glucose-6-phosphate dehydrogenase decreased 17β-HSD3 activity, indicating dependence on cytoplasmic NADPH. Upon selective permeabilization of the plasma membrane by digitonin, 17β-HSD3 but not 11β-HSD1 was detected by antibodies against C-terminal epitope tags, suggesting a cytoplasmic orientation of 17β-HSD3. The cytoplasmic orientation was confirmed using proteinase K digestion of microsomal preparations and by analysis of glycosylation of wild-type 17β-HSD3 and chimera in which the N-terminal anchor sequences between 17β-HSD3 and 11β-HSD1 were exchanged. In conclusion, the results demonstrate a cytoplasmic orientation of 17β-HSD3 and dependence on glucose-6-phosphate dehydrogenase-generated NADPH, explaining the lack of a direct functional coupling with the luminal 11β-HSD1-mediated glucocorticoid metabolism. **(*Endocrinology* 154: 205–213, 2013)**

Androgens play a key role in the regulation of male sexual development. In the testis, the conversion of the weak androgen Δ4-androstene-3,17-dione (AD) to the potent androgen testosterone is catalyzed by 17β-hydroxysteroid dehydrogenase 3 (17β-HSD3) (1). The formation of testosterone is essential for further activation by 5α-reductase, leading to the most potent androgen dihydrotestosterone, and also for generation of estradiol by aromatase. In humans and rodents, 17β-HSD3 is highly expressed in testis and at a lower level in other tissues, including prostate, bone, and adipose (1–3). The consequences of impaired 17β-HSD3 function are seen in patients with loss-of-function mutations who suffer from male pseudohermaphroditism (1, 4). In addition to genetic defects, 17β-HSD3 activity may be decreased by the presence of environmental chemicals or endogenous modulators that either directly inhibit enzyme activity or suppress its expression (5–8).

Glucocorticoids are important modulators of androgen action. Elevated glucocorticoid levels caused by stress

ISSN Print 0013-7227 ISSN Online 1945-7170
Printed in U.S.A.

doi: 10.1210/en.2012-1778 Received July 26, 2012. Accepted October 26, 2012.
First Published Online November 26, 2012

Abbreviations: AD, Δ4-Androstene-3,17-dione; ER, endoplasmic reticulum; G6PDH, glucose-6-phosphate dehydrogenase; GR, glucocorticoid receptor; HEK, human embryonic kidney; 11β-HSD1, 11β-hydroxysteroid dehydrogenase 1; 11β-HSD2, 17β-hydroxysteroid dehydrogenase 2; 17β-HSD3, 17β-hydroxysteroid dehydrogenase 3; H6PDH, hexose-6-phosphate dehydrogenase; MOPS, 3[*N*-morholino]propanesulfonic acid; $NADP^+$, oxidized nicotinamide adenine dinucleotide diphosphate; NAPDH, reduced nicotinamide adenine dinucleotide phosphate; NAPS, sodium phosphate and sucrose; PNGaseF, peptide-*N*-glycosidase F; siRNA, small interfering RNA; TLC, thin-layer chromatography.

have been associated with reduced male fertility in humans and rodents (9–11), with a negative correlation between circulating glucocorticoid and testosterone concentrations (12–15). Experiments with isolated rat Leydig cells showed that glucocorticoids can directly inhibit testosterone synthesis by a glucocorticoid receptor (GR)-dependent mechanism (16, 17).

Recently a functional coupling between 17β-HSD3 and the glucocorticoid-metabolizing enzyme 11β-hydroxysteroid dehydrogenase 1 (11β-HSD1) was proposed as a possible mechanism by which glucocorticoids might interfere with testosterone production in Leydig cells (18, 19). 11β-HSD1 catalyzes the oxoreduction of inactive 11-ketoglucocorticoids (cortisone, 11-dehydrocorticosterone) into their active forms (cortisol, corticosterone) and some other carbonyl containing steroidal and nonsteroidal compounds into their respective hydroxyl forms (20). 11β-HSD1 has been shown to function predominantly as a reductase in intact hepatocytes, adipocytes, and macrophage (21–23). Controversial observations were reported for the reaction direction in Leydig cells (24–26). Recently some investigators proposed that 11β-HSD1 may function as a dehydrogenase, thereby generating reduced nicotinamide adenine dinucleotide phosphate (NADPH) upon cortisol/corticosterone oxidation and stimulating 17β-HSD3-dependent reduction of AD (18, 19). This hypothesis implies that 11β-HSD1 and 17β-HSD3 are both localized within the endoplasmic reticulum (ER) and are dependent on the luminal NADPH/oxidized nicotinamide adenine dinucleotide phosphate ($NADP^+$) pool.

We and others demonstrated that 11β-HSD1 has a single N-terminal transmembrane helix and that the catalytic moiety faces the ER-lumen (27–30). Importantly, the oxoreductase activity of 11β-HSD1 depends on NADPH supply in the ER-lumen by hexose-6-phosphate dehydrogenase (H6PDH) (31–33). Because the ER membrane has a very low permeability for pyridine nucleotides, the luminal NADPH/$NADP^+$ pool is independent of that in the cytoplasm, and its ratio determines the reaction direction of 11β-HSD1 and other luminal enzymes using NADPH. H6PDH is fueled by glucose-6-phosphate via a glucose-6-phosphate transporter in the ER membrane or, alternatively, by fructose-6-phosphate, which can be converted to glucose-6-phosphate in the ER by an enzyme that remains to be identified (34).

The hypothesized functional coupling between 17β-HSD3 and 11β-HSD1 is based on the assumption that the catalytic domain of 17β-HSD3 is oriented toward the ER-lumen. Mindnich *et al.* (35) assigned the intracellular localization of 17β-HSD3 to the ER membrane; however, they did not solve its membrane topology. Here we investigated a potential functional coupling between 17β-HSD3 and 11β-HSD1 by using mouse MA-10 Leydig cells expressing endogenous levels of the two enzymes as well as transfected human embryonic kidney (HEK)-293 cells. We studied the dependence of the two enzymes on luminal and cytoplasmic NADPH and determined the membrane topology of 17β-HSD3.

Materials and Methods

Materials

Cell culture media, oligo-deoxythymidine, and Superscript II reverse transcriptase were purchased from Invitrogen (Carlsbad, CA); AD and [1,2-^{3}H]-cortisone from American Radiolabeled Chemicals (St. Louis, MO); and other steroids from Steraloids (Newport, RI). SIL G-25 UV254 thin-layer chromatography (TLC) plates were purchased from Macherey-Nagel (Oensingen, Switzerland). All other chemicals were from Fluka AG (Buchs, Switzerland).

Expression constructs

The plasmid for expression of C-terminally myc epitope-tagged 17β-HSD3 was constructed by PCR using a forward primer containing a *Bam*HI restriction endonuclease site followed by a Kozak consensus sequence (36) upstream of the ATG to initiator codon (5′-ATCGGATCCGCCATGGGGGACGTCCTGGAAC-3′) and a reverse primer containing a myc epitope tag for facilitated detection at the C terminus followed by the stop codon and a *Xba*I restriction endonuclease site (5′-ACTTCTAGATCAATCATC ATCATCTTTATAATCCATACCTGAACCCCTGACCTTGG TGTTGAGCTTCAG-3′) (5). Attachment of the C-terminal myc epitope did not affect enzyme activity. The chimeric constructs, in which the N-terminal transmembrane segment was exchanged, were obtained by PCR amplification. Sequences were exchanged at the beginning of the conserved Rossmann-fold at residue Lys36 of 11β-HSD1 and at Lys37 of 17β-HSD3. Chimeric construct N17–11HSD1 containing amino acids 1–36 of 17β-HSD3 followed by amino acids 36–292 of 11β-HSD1 was obtained using the forward primer 5′-GAGGATCCGCCATG GGGGACGTCCTGGAACAGTTCTTCATCCTCACAGGGC TGCTGGTGTGCCTGGCCTGCCTGGCGAAGTGCGTGAG ATTCTCCAGATGTGTTTTACTGAACTACTGGAAAGTGA TTGTCACAGGGGCCAGCAAAGG-3′ and the reverse primer 5′-GTTTCTAGACTAATCATCATCATCTTTATAATCCATTCC GCTTCCGCTTCCGCTTCCGCTTCCGCTTCCGCTTCCGCTT CCGCTTCCGCTTCCGCTCTTGTTTATGAATCTGTCCATAT TATAGCTCG-3′. Chimeric construct N11–17HSD3 containing amino acids 1–35 of 11β-HSD1 followed by amino acids 37–310 of 17β-HSD3 was obtained using the forward primer 5′-GAGGATCC GCCATGGCTTTTATGAAAAAATATCTCCTCCCCATTCTGG GGCTCTTCATGGCCTACTACTACTATTCTGCAAACGAGGA ATTCAGACCAGAGATGCTCCAAGGAAAGAAAGTTTTGCCA AAGTCTTTCTTGCGG-3′ and the reverse primer 5′-GTTTCTAG ACTAATCATCATCATCTTTATAATCCATTCCGCTTCCGCTT CCGCTTCCGCTTCCGCTTCCGCTTCCGCTTCCGCTTCCGC TTCCGCTCCTGACCTTGGTGTTGAGCTTCAGG-3′. The chimeric proteins were tagged with a FLAG-epitope at the C terminus to allow facilitated detection. All constructs were verified by sequencing.

Cell culture and transfection

HEK-293 cells were grown in DMEM supplemented with 10% fetal calf serum, 4.5 g/liter glucose, 50 U/ml penicillin/streptomycin, 2 mM glutamine, and 10 mM HEPES (pH 7.4). The mouse Leydig cell line MA-10 [kindly provided by Professor Mario Ascoli, University of Iowa, Iowa City, IA(37)] was cultivated on 0.1% gelatin-coated cell culture dishes in DMEM/F12 medium containing 20 mM HEPES (pH 7.4), 15% horse serum, and 50 μg/ml gentamicin. MA-10 cells were transfected using Lipofectamine reagent as described by the manufacturer (Life Technologies, Zug, Switzerland).

Measurement of 17β-HSD3 and 11β-HSD1 enzyme activity

Endogenous 17β-HSD3 activity of MA-10 cells was measured by incubating cells in serum- and steroid-free (doubly charcoal treated) DMEM/F12 medium containing 200 nM [1,2,6,7-^{3}H]-AD for 2–4 h. Reactions were terminated by adding 2 mM unlabeled AD and testosterone dissolved in methanol. Steroids were extracted with ethylacetate and separated on plastic coated UV-sensitive silica TLC plates using chloroform-methanol at a ratio of 9:1 as solvent system. Bands corresponding to the respective steroid were excised and transferred to tubes containing scintillation cocktail, and radioactive decay was analyzed on a β-counter. The percentage of conversion was obtained by dividing product counts by total counts. Quenching of the scintillation by the added plastic/silica matrix was less than 2%.

Endogenous 11β-HSD1 activity in intact MA-10 cells was determined by adding radiolabeled cortisone at a final concentration of 200 nM. After incubation at 37 C for 12–24 h, the amount of converted cortisone was assessed by ethylacetate extraction of steroids from the medium, TLC separation and scintillation counting.

Activities of recombinant enzymes expressed in HEK-293 cells were measured essentially as described earlier (5, 31). Cells were transiently transfected by the calcium-phosphate precipitation method with human recombinant 11β-HSD1 or 17β-HSD3, containing a C-terminal FLAG or myc epitope, respectively. The rates of conversion of cortisone to cortisol and AD to testosterone were determined. Reactions were terminated after 6 h by adding 2 mM unlabeled cortisol and cortisone and after 90 min by adding 2 mM unlabeled AD and testosterone dissolved in methanol.

The data were analyzed using multiple unpaired *t* tests, with Benjamini Hochberg FDR multiple testing correction (*, $P < 0.05$; **, $P < 0.01$; ***, $P < 0.001$).

Down-regulation of H6PDH and glucose-6-phosphate dehydrogenase (G6PDH) by small interfering RNA (siRNA)

MA-10 cells were cultured in 12-well plates. Cells were transfected with 20 nM of H6PDH siRNA (QIAGEN, Valencia, CA; Entrez Gene ID: 100198) or G6PDH siRNA (Dharmacon, Lafayette, CO; Entrez Gene ID: 2539) and retransfected with another 20 nM siRNA after 24 h. At 48 h after transfection, total RNA was extracted from adherent cells using Trizol reagent, followed by reverse transcriptase using Superscript II reverse transcriptase (Invitrogen). The mRNA levels were analyzed on a Rotor-Gene 6000 light cycler (Sydney, Australia). Reactions were performed in a total volume of 10 μl containing 20 ng cDNA, KAPA SYBR master mix (Kapasystems, Boston, MA) and specific primers and probes from Assay on Demand (Invitrogen). Expression levels relative to that of the internal control glyceraldehyde-3-phosphate dehydrogenase were determined using the $\Delta\Delta C_T$-method. H6PDH and G6PDH mRNA levels were decreased by 73 and 70%, respectively. Transfection of cells with scrambled control siRNA did not affect H6PDH and G6PDH mRNA expression. Enzyme activities were measured as described above. Experiments were performed in triplicates, with at least three independent experiments.

Selective permeabilization and immunofluorescence analysis

For immunofluorescence analysis, HEK-293 cells were transfected with the corresponding construct, fixed 48 h after transfection with 4% paraformaldehyde for 10 min, followed by washing three times with a buffer of 150 mM sodium phosphate (pH 7.4) and 120 mM sucrose (NAPS), as described earlier with minor modifications (29). Cells were incubated in blocking solution (NAPS containing 3% fetal bovine serum) for 30 min. For complete permeabilization of membranes, cells were incubated for another 30 min in blocking solution containing 0.5% Triton X-100. For selective permeabilization of the plasma membrane, cells were incubated for 1.5 min in blocking solution containing 25 μM digitonin. After washing three times with NAPS, cells were incubated in blocking solution (NAPS containing 3% fetal bovine serum) for 30 min. Enzymes were detected upon incubation with mouse monoclonal anti-FLAG antibody and rabbit polyclonal antimyc antibody overnight at 4 C, followed by three times washing, and incubation for 1 h at 25 C with ALEXA-488 goat antimouse and ALEXA-594 goat antirabbit antibody (Life Technologies, Zug, Switzerland), respectively. After washing, samples were mounted and analyzed on an Olympus FV1000-IX81 confocal microscope (Olympus, Volketswil, Switzerland) or on a Cellomics high-content imaging system according to the manufacturer's protocol (Cellomics ThermoScientific, Pittsburgh, PA).

Preparation of microsomes

HEK-293 cells (five 10 cm dishes each transfected with 5 μg of the corresponding expression plasmid) were collected 48 h after transfection, washed twice with PBS, and resuspended in 1.5 ml of ice-cold lysis buffer [10 mM 3[*N*-morholino]propanesulfonic acid (MOPS), pH 7.5; 0.5 mM $MgCl_2$; and Complete protease inhibitor (Roche Diagnostics, Rotkreuz, Switzerland)] and kept on ice for 5 min for cell lysis. The lysate was transferred into a Potter-Elvehjem homogenizer (Gerber Instruments, Effretikon, Switzerland). Samples were homogenized by 20 strokes, followed by addition of 2 ml of solution A (0.5 M sucrose; 10 mM MOPS, pH 7.5; 20 mM NaCl; 100 mM KCl; 1 mM dithiothreitol) and centrifugation at 11,000 $\times$ *g* for 15 min at 4 C. The supernatant was transferred into a new tube and centrifuged at 8800 $\times$ *g* for 20 min at 4 C. After centrifugation of the supernatant at 100,000 $\times$ *g* for 1 h at 4 C, the pellet was resuspended in 500 μl of buffer A and centrifuged again at 100,000 $\times$ *g* for 1 h at 4 C. The washed microsomal pellet fraction was resuspend in buffer B containing 10 mM MOPS (pH 7.5), 250 mM sucrose, 10 mM NaCl, 50 mM KCl, and 0.5 mM dithiothreitol. The protein concentration was determined by bicinchoninic assay protein detection assay. Microsomal preparations were shock frozen and

stored at −70 C until analysis. The described procedure yields almost exclusively inside-out microsomal vesicles (34), *i.e.* the cytoplasmic side is exposed to the aqueous solution and the ER-lumenal side is protected by the microsomal membrane.

Proteinase K protection assay and immunoblotting

The proteinase K protection assay was performed as described earlier (29). Microsomes (30 μg of total proteins) were incubated in a total volume of 25 μl with 0.5 μg/μl of proteinase K (Roche Diagnostics) for 15 min on ice in the presence or absence of 0.5% Triton X-100. Proteinase K was inactivated by adding 0.6 μl of 200 mM phenylmethylsulfonyl fluoride in isopropyl alcohol solution for 2 min, followed by adding SDS-PAGE sample buffer and immediate boiling for 5 min. Proteins were subjected to SDS-PAGE and Western blot analysis using anti-FLAG antibody M2 or antimyc antibody as primary antibodies and horseradish peroxidase-conjugated secondary antibody.

Deglycosylation assay

For deglycosylation of luminal proteins, microsomes (5 μg total proteins) were permeabilized with 0.5% Triton X-100, followed by boiling for 10 min in glycoprotein denaturation buffer. After cooling, microsomes were incubated for 1 h at 37 C in a final volume of 20 μl containing 500 U of peptide-*N*-glycosidase F (PNGaseF; New England Biolabs, Beverly, MA). The reaction was stopped by adding SDS-PAGE sample buffer, and samples were analyzed by SDS-PAGE and subsequent immunoblotting.

Results

Lack of a direct functional interaction between 17β-HSD3 and 11β-HSD1

The hypothesized functional interaction between 17β-HSD3 and 11β-HSD1, by competing for the same NADPH/$NADP^+$ pool, is based on the assumption of a luminal orientation of the catalytic moiety of 17β-HSD3. To test the existence of a functional coupling between the two enzymes, we coexpressed 17β-HSD3 and 11β-HSD1 either alone or in combination in HEK-293 cells and measured the respective enzyme activity. To assure that the transfected cells indeed coexpress FLAG-tagged 11β-HSD1 and myc-tagged 17β-HSD3, we analyzed the expression of each enzyme by confocal microscopy. In total, approximately 30% of cells were transfected, whereby 82% expressed both enzymes, 10% expressed myc-tagged 17β-HSD3 only, and 8% expressed 11β-HSD1 only. Similar coexpression experiments in HEK-293 cells were previously performed to demonstrate the functional impact of H6PDH on 11β-HSD1 (32). Thus, coexpression of both enzymes in HEK-293 cells should potentially reveal a functional interaction if it exists.

At a physiologically relevant concentration of 200 nM, neither cortisone nor cortisol affected the 17β-HSD3-dependent conversion of AD to testosterone upon incuba-

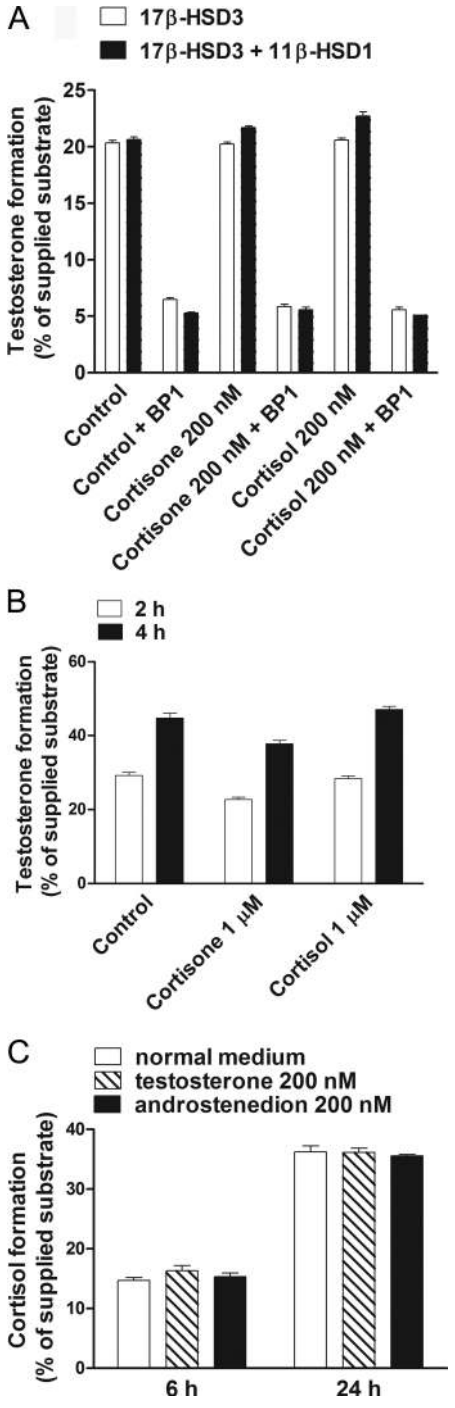

FIG. 1. 17β-HSD3 and 11β-HSD1 do not functionally interact in MA-10 cells and in transfected HEK-293 cells. A, HEK-293 cells were transfected with 17β-HSD3 alone or together with 11β-HSD1. At 48 h after transfection, 17β-HSD3-dependent conversion of 200 nM AD to testosterone (90 min incubation) was determined in the presence of vehicle, 200 nM cortisone or cortisol, and 5 μM of the 17β-HSD3 inhibitor benzophenone-1 (BP1), respectively. B, 17β-HSD3-dependent conversion of 200 nM AD to testosterone (2 and 4 h incubation) was determined in MA-10 mouse Leydig cells in the absence or presence of 1 μM cortisone or cortisol. C, HEK-293 cells were transfected with 11β-HSD1, followed by measuring the conversion of 200 nM cortisone to cortisol (incubation 6 and 24 h) in the presence of vehicle, 200 nM testosterone, or 200 nM AD. Data represent mean ± SD from three independent experiments.

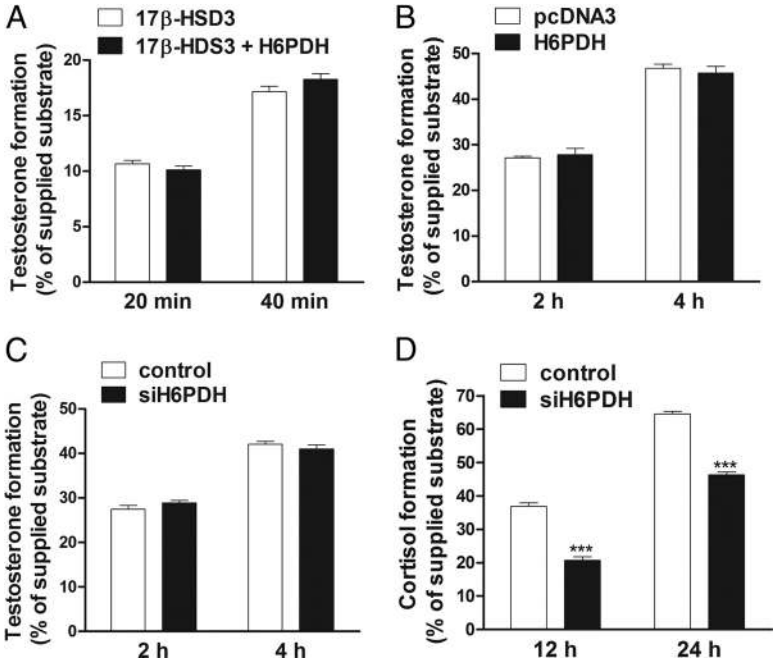

FIG. 2. Coexpression with H6PDH does not affect 17β-HSD3 activity. A, HEK-293 cells were transfected with 17β-HSD3 and either pcDNA3 vector control or H6PDH. At 48 h after transfection, 17β-HSD3-dependent reduction of AD (200 nM) to testosterone was measured for 20 and 40 min. B, MA-10 cells with endogenous 17β-HSD3 expression were transfected with pcDNA3 control or H6PDH. Conversion of AD (200 nM) to testosterone was determined after 2 and 4 h. To investigate the impact of H6PDH knockdown, MA-10 cells were transfected with scrambled control siRNA or siRNA against H6PDH. At 48 h after the transfection, 17β-HSD3 activity (C) and 11β-HSD1 (D) was determined. Data represent mean ± SD from three independent experiments. ***, $P < 0.001$.

tion for 90 min in cells expressing 17β-HSD3 alone or upon coexpression with 11β-HSD1 (Fig. 1A). Also, inhibition of 17β-HSD3 by the known inhibitor benzophenone-1 (*5*) was not affected upon coexpression with 11β-HSD1. Similar observations were made in MA-10 mouse Leydig cells expressing endogenous levels of the two enzymes (Fig. 1B). Due to the longer incubation time (2 and 4 h), 1 μM of cortisone and cortisol was used to avoid a substantial decrease in concentrations due to metabolism. Similarly, at 200 nM final concentration, neither AD nor testosterone affected the 11β-HSD1-dependent reduction of cortisone in HEK-293 cells in the presence or absence of 17β-HSD3 (Fig. 1C).

H6PDH does not modulate 17β-HSD3 activity

To investigate the impact of H6PDH on 17β-HSD3 activity, we expressed 17β-HSD3 in the absence or presence of H6PDH in HEK-293 cells and determined the conversion of AD to testosterone. Coexpression with H6PDH did not affect 17β-HSD3 activity (Fig. 2A). We also tested whether overexpression of H6PDH in MA-10 cells might affect the activity of endogenous 17β-HSD3 (Fig. 2B). The fact that we could not detect an increased 17β-HSD3 activity might be due to substantial endogenous H6PDH expression. Therefore, we treated MA-10 cells with siRNA against H6PDH. The 17β-HSD3-dependent reduction of AD was not altered (Fig. 2C); however, the 11β-HSD1-dependent reduction of cortisone was significantly decreased, as expected (Fig. 2D). These experiments suggested that 17β-HSD3 either has a luminal orientation but is independent of H6PDH-generated NADPH or that it is oriented toward the cytoplasm.

Determination of the membrane topology of 17β-HSD3

To determine the orientation in the ER membrane of 17β-HSD3, we transfected HEK-293 cells with C-terminally myc epitope-tagged 17β-HSD3 and analyzed the intracellular localization by fluorescence microscopy. As controls, FLAG-tagged 11β-hydroxysteroid dehydrogenase 2 (11β-HSD2) (with cytoplasmic orientation) and myc-tagged H6PDH (with luminal localization) were used. Analysis of 5000 cells per well and measurement by Cellomics ArrayScan high-content imaging revealed a transfection rate of approximately 30%, with comparable numbers of positive signals for 17β-HSD3 upon selective permeabilization of the plasma membrane with 25 μM digitonin and complete permeabilization using 0.5% Triton X-100 (Fig. 3A). These observations indicated that the catalytic moiety of 17β-HSD3 protrudes into the cytoplasm. 11β-HSD2 and H6PDH showed cytoplasmic and luminal orientation, respectively, as previously reported (27, 32). To assess the role of the N-terminal transmembrane helix, we constructed two chimeric proteins. N17–11HSD1 consisted of the N-terminal membrane anchor of 17β-HSD3, followed by the cytoplasmic moiety of 11β-HSD1. N11–17HSD3 had the N-terminal helix of 11β-HSD1 fused to the catalytic domain of 17β-HSD3. As shown in Fig. 3A, the C-terminal tag of N17–11HSD1 was accessible to antibody in digitonin-treated cells, whereas N11–17HSD3 was protected. Thus, the N-terminal transmembrane sequence of 17β-HSD3 and 11β-HSD1 determines the cytoplasmic and luminal orientation, respectively. In addition to high-content imaging, cells treated with either Triton X-100 or digitonin were also analyzed by confocal microscopy by counting fluorescence positive cells among 500 cells randomly chosen in phase contrast. Despite differences in the transfection rates and/or threshold of fluorescence detection with the different constructs, similar rates of positive cells than with high-content imaging were obtained (Table 1).

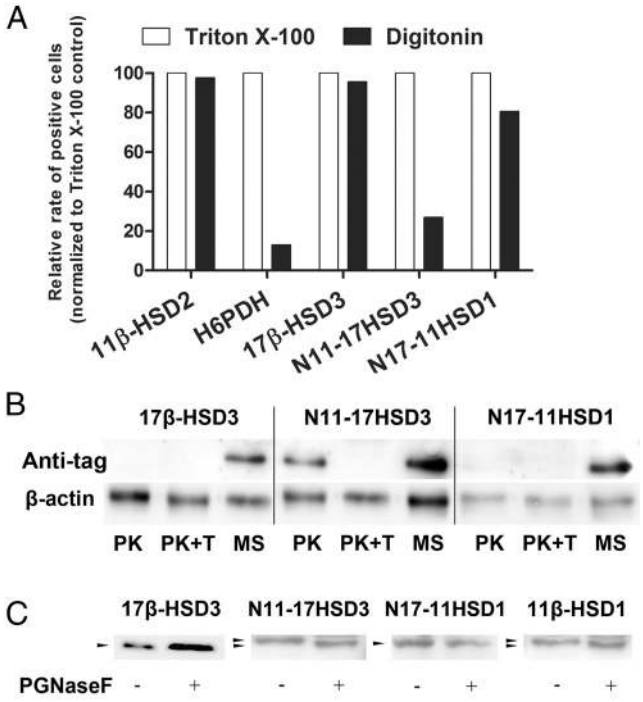

FIG. 3. Determination of the membrane topology of 17β-HSD3. HEK-293 cells were transfected with different constructs. A, After 48 h, cells were fixed with 4% paraformaldehyde, followed by blocking for 30 min and selective permeabilization of the plasma membrane by incubation with 25 μM digitonin for 1.5 min or full permeabilization of membranes by incubation with 0.5% Triton X-100 for 30 min. Fluorescence was analyzed using Cellomics ArrayScan high-content screening system by staining nuclei with Hoechst 33342 and counting cells yielding a positive signal with the respective anti-tag antibody. Results were normalized to Triton X-100-positive control. B, Microsomal preparations of cells expressing the respective C-terminally myc- or FLAG-tagged wild-type or chimeric protein were analyzed before any treatment (MS) or after incubation for 15 min on ice with 0.5 μg/μl proteinase K in the absence (PK) or presence of 0.5% Triton X-100 (PK + T). Proteins were analyzed by Western blotting using mouse monoclonal anti-tag antibody and secondary antimouse horseradish peroxidase antibody. C, For deglycosylation of proteins, microsomes were incubated with 500 U of PNGaseF for 1 h at 37 C, followed by analysis of samples by SDS-PAGE and Western blotting. Representative experiments are shown. N11–17HSD3, Chimera consisting of the N-terminal membrane anchor of 11β-HSD1 and the catalytic moiety of 17β-HSD3; N17–11HSD1, chimera consisting of the N-terminal membrane anchor of 17β-HSD3 and the catalytic moiety of 11β-HSD1. 11β-HSD1, 11β-HSD2, N11–17HSD3, and N17–11HSD1 have a C-terminal FLAG-tag. 17β-HSD3 and H6PDH have a C-terminal myc-tag.

To confirm the membrane topology of 17β-HSD3 and the chimeric proteins, we incubated microsomal vesicles expressing the respective protein for 15 min with proteinase K in the absence or presence of 0.5% Triton X-100. In the absence of detergent, the chimera N11–17HSD3 was protected from degradation by proteinase K, as expected (Fig. 3B). 11β-HSD1 and H6PDH were also protected from degradation [not shown (27)]. In contrast, both 17β-HSD3 and N17–11HSD1 were readily degraded, indicating cytoplasmic orientation. Additionally, because luminal but not cytoplasmic proteins can be glycosylated, we employed a deglycosylation assay. Treatment of microsomal preparations with PNGaseF for 1 h at 37 C did not alter the mobility of 17β-HSD3 and N17–11HSD1 protein on SDS-PAGE but led to a band that migrated faster in case of H6PDH (not shown), 11β-HSD1, and N11–17HSD3 (Fig. 3C).

Glucose and cytoplasmic NADPH generation stimulate testosterone formation in MA-10 Leydig cells

A cytoplasmic orientation of 17β-HSD3 implies a dependence of the enzyme on the cytoplasmic NADPH pool. To test this assumption, we incubated MA-10 cells in normal medium containing 1 g/liter glucose and in low-glucose (0.1 g/liter) medium. A significantly decreased 17β-HSD3-dependent testosterone formation was found under low glucose conditions (Fig. 4). Moreover, knockdown of the cytoplasmic NADPH-generating enzyme G6PDH by siRNA significantly reduced 17β-HSD3 activity, an effect that was more pronounced under low-glucose conditions in which cytoplasmic glucose-6-phosphate production is less efficient.

Discussion

In the present study, we could not observe a functional coupling between 17β-HSD3 and 11β-HSD1. Coexpression with 11β-HSD1 and/or the addition of glucocorticoids did not alter 17β-HSD3 activity. Furthermore, 17β-HSD3-dependent reduction of AD was not affected by overexpression or knockdown of the luminal NADPH generating H6PDH, but it was decreased by knockdown of the cytoplasmic NADPH source G6PDH, suggesting cytoplasmic orientation of 17β-HSD3.

The intracellular localization of human and zebrafish 17β-HSD3 has been localized to the ER (35); however, the membrane topology was not resolved. Using selective permeabilization of the plasma membrane, proteinase K digestion, and analysis of glycosylation patterns of wild-type and chimeric enzymes, we demonstrate a cytoplasmic orientation of 17β-HSD3. Importantly, we could show that the N-terminal membrane anchor sequences of 17β-HSD3 and 11β-HSD1 are sufficient to determine their cytoplasmic and luminal orientation, respectively. This resembles previous observations with 11β-HSD2 (27), Rdh1, and Crad1 (38). Thus, 17β-HSD3 and 11β-HSD1 are facing different compartments and use distinct NADPH pools (Fig. 5).

TABLE 1. Topology of 17β-HSD3, chimeric proteins, and controls

Expressed protein	Triton X-100	Digitonin	Relative rate of positive cells with digitonin
11β-HSD2, C-terminal FLAG	27 ± 2	26 ± 2	96 ± 2
H6PDH, C-terminal myc	23 ± 2	2 ± 1	9 ± 1
17β-HSD3, C-terminal myc	18 ± 1	15 ± 1	84 ± 1
N11-17HSD3, C-terminal FLAG	22 ± 3	5 ± 1	26 ± 2
N17-11HSD1, C-terminal FLAG	26 ± 2	18 ± 1	72 ± 1

Transfected HEK-293 cells were either fully permeabilized with 0.5% Triton X-100 or the plasma membrane was selectively permeabilized with 25 μM digitonin, allowing restricted access of the antibody to the cytosolic compartment. Cells were incubated with primary anti-tag and fluorescence-labeled secondary antibody, followed by analysis of fluorescent cells using confocal microscopy. *Numbers* represent the percentage of fluorescent cells relative to total cells from three independent experiments. In each experiment 500 cells were counted. Data represent mean ± SD.

That 17β-HSD3 is dependent on cytoplasmic and not luminal NADPH is supported by the fact that both H6PDH-deficient mice and H6PDH/11β-HSD1 double knockout mice are fertile and do not seem to have impaired male development (39–41). Patients with cortisone reductase deficiency have increased rather than decreased androgen production (42), indicating that 17β-HSD3 function is not abolished by impaired H6PDH/11β-HSD1 activity.

The present study emphasizes the importance of the knowledge of intracellular localization and membrane topology to understand enzyme function. Nevertheless, this information is available only for very few of the microsomal short-chain dehydrogenase/reductase enzymes (43, 44), and resolving the membrane topology might provide further insight into the physiological roles of these enzymes.

To further study a potential interference of glucocorticoids with 17β-HSD3-dependent testosterone formation, we recently began to investigate its transcriptional regulation. Despite the known suppressive effect of elevated glucocorticoids on testosterone production by Leydig cells, incubation of MA-10 Leydig cells with 100 nM of the potent glucocorticoid dexamethasone did not affect 17β-HSD3 mRNA expression. Expression of the GR was verified by RT-PCR. Furthermore, 100 nM dexamethasone did not alter *HSD17B3* promoter-driven luciferase reporter expression in HEK-293 cells cotransfected with GR (data not shown). Therefore, the suppressive effect of glucocorticoids on androgen production is most likely caused by inhibition of steroidogenesis. Reduced expression of steroidogenic acute regulatory protein (45), cytochrome P450 side-chain cleavage enzyme (17), and cytochrome P450–17 (16) upon treatment with elevated glucocorticoids have been reported. Also, glucocorticoid-dependent apoptosis of testosterone producing Leydig cells has been reported (46, 47).

In conclusion, glucocorticoids do not seem to modulate 17β-HSD3 expression and activity. Reduced steroidogen-

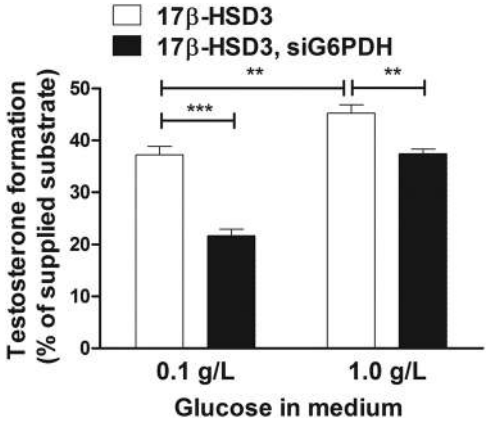

FIG. 4. Modulation of 17β-HSD3 activity by glucose and cytoplasmic NADPH. HEK-293 cells were transfected with 17β-HSD3 and either scrambled control siRNA or siRNA against the cytosolic NADPH generating enzyme G6PDH. Before incubation with the respective medium, the cells were preincubated with carbohydrate-free medium for 2 h, followed by incubation in low (0.1 g/liter) or high (1 g/liter) glucose medium and determination of 17β-HSD3 activity for 30 min at a supplied AD concentration of 200 nM.

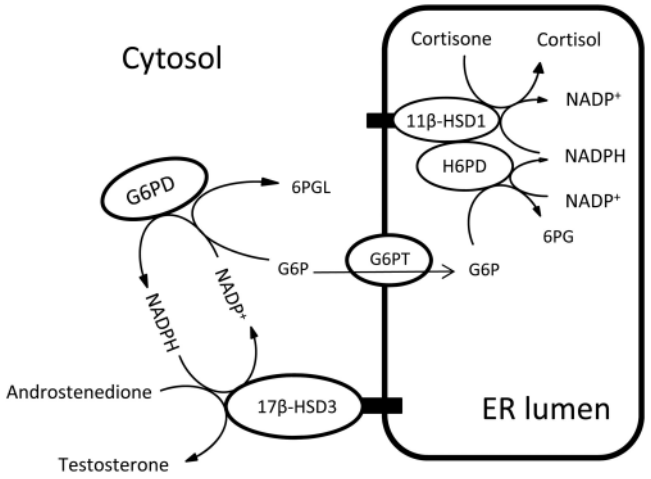

FIG. 5. Model of 17β-HSD3 and 11β-HSD1 localization and their respective NADPH-supplying enzymes. The cytoplasm and ER maintain independent NADPH/$NADP^+$ pools that are dependent on cytoplasmic G6PDH and luminal H6PDH, respectively. 17β-HSD3 is anchored by its N-terminal transmembrane helix in the ER membrane and protrudes into the cytoplasm, and its activity is stimulated by G6PDH-generated NADPH, whereas 11β-HSD1 faces the ER-lumen and interacts with the NADPH supplying H6PDH. G6P, Glucose-6-phosphate; G6PD, G6P dehydrogenase; G6PT, G6P (6-phosphogluconate) translocase of the ER membrane; H6PD, hexose-6-phosphate dehydrogenase.

esis may be responsible for the observed glucocorticoid-mediated suppression of androgen production.

Acknowledgments

We thank Carlos A. Penno for support with topology assays and Thierry Da Cunha for Cellomics.

Address all correspondence and requests for reprints to: Dr. Alex Odermatt, Division of Molecular and Systems Toxicology, Department of Pharmaceutical Sciences, University of Basel, Klingelbergstrasse 50, 4056 Basel, Switzerland. E-mail: alex.odermatt@unibas.ch.

This work was supported by the Swiss National Science Foundation (Grants 31003A-140961 and R'Equip. 316030-133859). A.O. has a Chair for Molecular and Systems Toxicology by the Novartis Research Foundation.

Disclosure Summary: The authors have nothing to disclose.

References

1. **Geissler WM, Davis DL, Wu L, Bradshaw KD, Patel S, Mendonca BB, Elliston KO, Wilson JD, Russell DW, Andersson S** 1994 Male pseudohermaphroditism caused by mutations of testicular 17β-hydroxysteroid dehydrogenase 3. Nat Genet 7:34–39
2. **Sha JA, Dudley K, Rajapaksha WR, O'Shaughnessy PJ** 1997 Sequence of mouse 17β-hydroxysteroid dehydrogenase type 3 cDNA and tissue distribution of the type 1 and type 3 isoform mRNAs. J Steroid Biochem Mol Biol 60:19–24
3. **Mustonen MV, Poutanen MH, Isomaa VV, Vihko PT, Vihko RK** 1997 Cloning of mouse 17β-hydroxysteroid dehydrogenase type 2, and analysing expression of the mRNAs for types 1, 2, 3, 4 and 5 in mouse embryos and adult tissues. Biochem J 325(Pt 1):199–205
4. **Andersson S, Geissler WM, Wu L, Davis DL, Grumbach MM, New MI, Schwarz HP, Blethen SL, Mendonca BB, Bloise W, Witchel SF, Cutler Jr GB, Griffin JE, Wilson JD, Russel DW** 1996 Molecular genetics and pathophysiology of 17β-hydroxysteroid dehydrogenase 3 deficiency. J Clin Endocrinol Metab 81:130–136
5. **Nashev LG, Schuster D, Laggner C, Sodha S, Langer T, Wolber G, Odermatt A** 2010 The UV-filter benzophenone-1 inhibits 17β-hydroxysteroid dehydrogenase type 3: virtual screening as a strategy to identify potential endocrine disrupting chemicals. Biochem Pharmacol 79:1189–1199
6. **Lo S, Alléra A, Albers P, Heimbrecht J, Jantzen E, Klingmüller D, Steckelbroeck S** 2003 Dithioerythritol (DTE) prevents inhibitory effects of triphenyltin (TPT) on the key enzymes of the human sex steroid hormone metabolism. J Steroid Biochem Mol Biol 84:569–576
7. **Ohno S, Nakajima Y, Nakajin S** 2005 Triphenyltin and tributyltin inhibit pig testicular 17β-hydroxysteroid dehydrogenase activity and suppress testicular testosterone biosynthesis. Steroids 70:645–651
8. **Yuan K, Zhao B, Li XW, Hu GX, Su Y, Chu Y, Akingbemi BT, Lian QQ, Ge RS** 2012 Effects of phthalates on 3β-hydroxysteroid dehydrogenase and 17β-hydroxysteroid dehydrogenase 3 activities in human and rat testes. Chem Biol Interact 195:180–188
9. **Orr TE, Mann DR** 1990 Effects of restraint stress on plasma LH and testosterone concentrations, Leydig cell LH/hCG receptors, and *in vitro* testicular steroidogenesis in adult rats. Horm Behav 24:324–341
10. **Orr TE, Mann DR** 1992 Role of glucocorticoids in the stress-induced suppression of testicular steroidogenesis in adult male rats. Horm Behav 26:350–363
11. **Fenster L, Katz DF, Wyrobek AJ, Pieper C, Rempel DM, Oman D, Swan SH** 1997 Effects of psychological stress on human semen quality. J Androl 18:194–202
12. **Smals AG, Kloppenborg PW, Benraad TJ** 1977 Plasma testosterone profiles in Cushing's syndrome. J Clin Endocrinol Metab 45:240–245
13. **Nakashima A, Koshiyama K, Uozumi T, Monden Y, Hamanaka Y** 1975 Effects of general anaesthesia and severity of surgical stress on serum LH and testosterone in males. Acta Endocrinol (Copenh) 78:258–269
14. **Monder C, Sakai RR, Miroff Y, Blanchard DC, Blanchard RJ** 1994 Reciprocal changes in plasma corticosterone and testosterone in stressed male rats maintained in a visible burrow system: evidence for a mediating role of testicular 11β-hydroxysteroid dehydrogenase. Endocrinology 134:1193–1198
15. **Hardy MP, Sottas CM, Ge R, McKittrick CR, Tamashiro KL, McEwen BS, Haider SG, Markham CM, Blanchard RJ, Blanchard DC, Sakai RR** 2002 Trends of reproductive hormones in male rats during psychosocial stress: role of glucocorticoid metabolism in behavioral dominance. Biol Reprod 67:1750–1755
16. **Orr TE, Taylor MF, Bhattacharyya AK, Collins DC, Mann DR** 1994 Acute immobilization stress disrupts testicular steroidogenesis in adult male rats by inhibiting the activities of 17α-hydroxylase and 17,20-lyase without affecting the binding of LH/hCG receptors. J Androl 15:302–308
17. **Hales DB, Payne AH** 1989 Glucocorticoid-mediated repression of P450scc mRNA and de novo synthesis in cultured Leydig cells. Endocrinology 124:2099–2104
18. **Hu GX, Lian QQ, Lin H, Latif SA, Morris DJ, Hardy MP, Ge RS** 2008 Rapid mechanisms of glucocorticoid signaling in the Leydig cell. Steroids 73:1018–1024
19. **Latif SA, Shen M, Ge RS, Sottas CM, Hardy MP, Morris DJ** 2011 Role of 11β-OH-C(19) and C(21) steroids in the coupling of 11β-HSD1 and 17β-HSD3 in regulation of testosterone biosynthesis in rat Leydig cells. Steroids 76:682–689
20. **Odermatt A, Nashev LG** 2010 The glucocorticoid-activating enzyme 11β-hydroxysteroid dehydrogenase type 1 has broad substrate specificity: physiological and toxicological considerations. J Steroid Biochem Mol Biol 119:1–13
21. **Balázs Z, Nashev LG, Chandsawangbhuwana C, Baker ME, Odermatt A** 2009 Hexose-6-phosphate dehydrogenase modulates the effect of inhibitors and alternative substrates of 11β-hydroxysteroid dehydrogenase 1. Mol Cell Endocrinol 301:117–122
22. **Jamieson PM, Chapman KE, Edwards CR, Seckl JR** 1995 11 β-Hydroxysteroid dehydrogenase is an exclusive 11β-reductase in primary cultures of rat hepatocytes: effect of physicochemical and hormonal manipulations. Endocrinology 136:4754–4761
23. **Thieringer R, Le Grand CB, Carbin L, Cai TQ, Wong B, Wright SD, Hermanowski-Vosatka A** 2001 11β-Hydroxysteroid dehydrogenase type 1 is induced in human monocytes upon differentiation to macrophages. J Immunol 167:30–35
24. **Ge RS, Hardy MP** 2000 Initial predominance of the oxidative activity of type I 11β-hydroxysteroid dehydrogenase in primary rat Leydig cells and transfected cell lines. J Androl 21:303–310
25. **Leckie CM, Welberg LA, Seckl JR** 1998 11β-Hydroxysteroid dehydrogenase is a predominant reductase in intact rat Leydig cells. J Endocrinol 159:233–238
26. **Ferguson SE, Pallikaros Z, Michael AE, Cooke BA** 1999 The effects of different culture media, glucose, pyridine nucleotides and adenosine on the activity of 11β-hydroxysteroid dehydrogenase in rat Leydig cells. Mol Cell Endocrinol 158:37–44
27. **Odermatt A, Arnold P, Stauffer A, Frey BM, Frey FJ** 1999 The N-terminal anchor sequences of 11β-hydroxysteroid dehydroge-

nases determine their orientation in the endoplasmic reticulum membrane. J Biol Chem 274:28762–28770
28. **Mziaut H, Korza G, Hand AR, Gerard C, Ozols J** 1999 Targeting proteins to the lumen of endoplasmic reticulum using N-terminal domains of 11β-hydroxysteroid dehydrogenase and the 50-kDa esterase. J Biol Chem 274:14122–14129
29. **Frick C, Atanasov AG, Arnold P, Ozols J, Odermatt A** 2004 Appropriate function of 11β-hydroxysteroid dehydrogenase type 1 in the endoplasmic reticulum lumen is dependent on its N-terminal region sharing similar topological determinants with 50-kDa esterase. J Biol Chem 279:31131–31138
30. **Ozols J** 1995 Lumenal orientation and post-translational modifications of the liver microsomal 11β-hydroxysteroid dehydrogenase. J Biol Chem 270:2305–2312
31. **Atanasov AG, Nashev LG, Gelman L, Legeza B, Sack R, Portmann R, Odermatt A** 2008 Direct protein-protein interaction of 11β-hydroxysteroid dehydrogenase type 1 and hexose-6-phosphate dehydrogenase in the endoplasmic reticulum lumen. Biochim Biophys Acta 1783:1536–1543
32. **Atanasov AG, Nashev LG, Schweizer RA, Frick C, Odermatt A** 2004 Hexose-6-phosphate dehydrogenase determines the reaction direction of 11β-hydroxysteroid dehydrogenase type 1 as an oxoreductase. FEBS Lett 571:129–133
33. **Bánhegyi G, Benedetti A, Fulceri R, Senesi S** 2004 Cooperativity between 11β-hydroxysteroid dehydrogenase type 1 and hexose-6-phosphate dehydrogenase in the lumen of the endoplasmic reticulum. J Biol Chem 279:27017–27021
34. **Senesi S, Legeza B, Balázs Z, Csala M, Marcolongo P, Kereszturi E, Szelényi P, Egger C, Fulceri R, Mandl J, Giunti R, Odermatt A, Bánhegyi G, Benedetti A** 2010 Contribution of fructose-6-phosphate to glucocorticoid activation in the endoplasmic reticulum: possible implication in the metabolic syndrome. Endocrinology 151:4830–4839
35. **Mindnich R, Haller F, Halbach F, Moeller G, Hrabé de Angelis M, Adamski J** 2005 Androgen metabolism via 17β-hydroxysteroid dehydrogenase type 3 in mammalian and non-mammalian vertebrates: comparison of the human and the zebrafish enzyme. J Mol Endocrinol 35:305–316
36. **Kozak M** 1987 At least six nucleotides preceding the AUG initiator codon enhance translation in mammalian cells. J Mol Biol 196:947–950
37. **Ascoli M** 1981 Regulation of gonadotropin receptors and gonadotropin responses in a clonal strain of Leydig tumor cells by epidermal growth factor. J Biol Chem 256:179–183
38. **Zhang M, Hu P, Napoli JL** 2004 Elements in the N-terminal signaling sequence that determine cytosolic topology of short-chain dehydrogenases/reductases: studies with retinol dehydrogenase type 1 and cis-retinol/androgen dehydrogenase type 1. J Biol Chem 279:51482–51489
39. **Lavery GG, Walker EA, Turan N, Rogoff D, Ryder JW, Shelton JM, Richardson JA, Falciani F, White PC, Stewart PM, Parker KL, McMillan DR** 2008 Deletion of hexose-6-phosphate dehydrogenase activates the unfolded protein response pathway and induces skeletal myopathy. J Biol Chem 283:8453–8461
40. **Semjonous NM, Sherlock M, Jeyasuria P, Parker KL, Walker EA, Stewart PM, Lavery GG** 2011 Hexose-6-phosphate dehydrogenase contributes to skeletal muscle homeostasis independent of 11β-hydroxysteroid dehydrogenase type 1. Endocrinology 152:93–102
41. **Lavery GG, Walker EA, Draper N, Jeyasuria P, Marcos J, Shackleton CH, Parker KL, White PC, Stewart PM** 2006 Hexose-6-phosphate dehydrogenase knock-out mice lack 11β-hydroxysteroid dehydrogenase type 1-mediated glucocorticoid generation. J Biol Chem 281:6546–6551
42. **Draper N, Walker EA, Bujalska IJ, Tomlinson JW, Chalder SM, Arlt W, Lavery GG, Bedendo O, Ray DW, Laing I, Malunowicz E, White PC, Hewison M, Mason PJ, Connell JM, Shackleton CH, Stewart PM** 2003 Mutations in the genes encoding 11β-hydroxysteroid dehydrogenase type 1 and hexose-6-phosphate dehydrogenase interact to cause cortisone reductase deficiency. Nat Genet 34:434–439
43. **Skarydová L, Wsól V** 2012 Human microsomal carbonyl reducing enzymes in the metabolism of xenobiotics: well-known and promising members of the SDR superfamily. Drug Metab Rev 44:173–191
44. **Bray JE, Marsden BD, Oppermann U** 2009 The human short-chain dehydrogenase/reductase (SDR) superfamily: a bioinformatics summary. Chem Biol Interact 178:99–109
45. **Wang X, Walsh LP, Reinhart AJ, Stocco DM** 2000 The role of arachidonic acid in steroidogenesis and steroidogenic acute regulatory (StAR) gene and protein expression. J Biol Chem 275:20204–20209
46. **Gao HB, Tong MH, Hu YQ, Guo QS, Ge R, Hardy MP** 2002 Glucocorticoid induces apoptosis in rat Leydig cells. Endocrinology 143:130–138
47. **Gao HB, Tong MH, Hu YQ, You HY, Guo QS, Ge RS, Hardy MP** 2003 Mechanisms of glucocorticoid-induced Leydig cell apoptosis. Mol Cell Endocrinol 199:153–163